Supplementary Information to the article:

"Moisture origin as a driver of temporal variabilities of the water vapour isotopic composition in the Lena River Delta, Siberia"

Supplementary Note 1 - Calibration of the water vapour isotopic analyser

The humidity concentration-dependence of the isotope measurements of the Picarro L2140-i instrument is corrected based on the measured isotopic composition over a range of different humidity values for each of four water standards. The results of the calibration measurements are presented in Supplementary Fig. 1. The temporal stability of this correction has been evaluated by successive measurements of this so-called humidity-response function at different times. No significant drift of this response was observed for any of the different standards, neither for successive measurements over a week (not presented in the graphics) nor for measurements separated by several months over the complete observational period (as shown by the different measurement sequences in the graphics). The humidity-response function is thus considered constant in time. It does, however, depend on the isotopic standard used. A humidity-response function is computed for each isotopic standard as the interpolation of the distribution of all experiments with a polynomial function of 4th order. The correction of the humidity-concentration dependence for a specific near-surface vapour measurement is determined by the linear interpolation of the two humidity-response functions from the closest surrounding isotopic standards at the isotopic value of the measurement.

Calibration curves are applied to correct from deviation of the raw instrument data from the VSMOW-SLAP scale. These calibration curves are calculated based on the repeated measurement of every liquid standard for 30 minutes every 25 hours (a standard measurements sequence consists in the successive measurement of all calibration standards). To avoid any memory effects, mean isotope values and standard deviations are computed over the last 15 minutes of each injection, only. Several filtration and correction steps are applied to these liquid standard measurements before computing the calibration curve. All measurements are corrected for the humidity-concentration dependence. To account for the difference in isotopic composition of the same liquid standard stored in different bottles and used on separate injection lines, we define an arbitrary reference standard among both bottles and correct the measured isotopic values from the difference between the known isotopic value of both bottles. We remove measurements with average H_2O values ($\overline{H_2O}$) below 5000 ppm or higher than 28000 ppm and standard deviations of H_2O , $\delta^{18}O$ or $\delta^{2}H$ (noted $\sigma(H_2O)$, $\sigma(\delta^{18}O)$, $\sigma(\delta^{2}H)$, respectively) higher than 2500 ppm, 1.5 ‰ and 5 ‰. For the standard measured with the bubbler, we remove data measured with a water temperature below 5°C. We compute a first 14-days running average and eliminate all measurements that deviate from this running average by more than 1.5 ‰, 5 ‰ and 8 ‰ for $\delta^{18}O$, $\delta^{2}H$ and d-excess, respectively. The observed variabilities of these selected measurements of all liquid standards are shown in Supplementary Fig. 2.

The calibration curves are calculated every time a standard measurements sequence has been performed, based on a new 14-days running average of the previously selected liquid standard measurements. These values are compared to the theoretical values of the reference standards at the time of the standard measurements sequence. If values of at least 3 standards are available, a linear regression of the measurements against the theoretical values gives the calibration curve. Otherwise, as found in literature for such type of analyzers, we correct the calibration curve from the drift of the running average of the standards which have been correctly measured and use an interpolated value of the slope between the closest calculated calibration curve. Such drift correction in cases were the slope cannot be calculated is similar to the procedure of Steen-Larsen et al. 2014.

References:

Steen-Larsen, H. C., A. E. Sveinbjörnsdottir, A. J. Peters, V. Masson-Delmotte, M. P. Guishard, G. Hsiao, J. Jouzel, D. Noone, J. K. Warren, and J. W. C. White. 2014. “Climatic Controls on Water Vapor Deuterium Excess in the Marine Boundary Layer of the North Atlantic Based on 500 Days of in Situ, Continuous Measurements.” *Atmos. Chem. Phys.* 14 (15): 7741–56. https://doi.org/10.5194/acp-14-7741-2014.

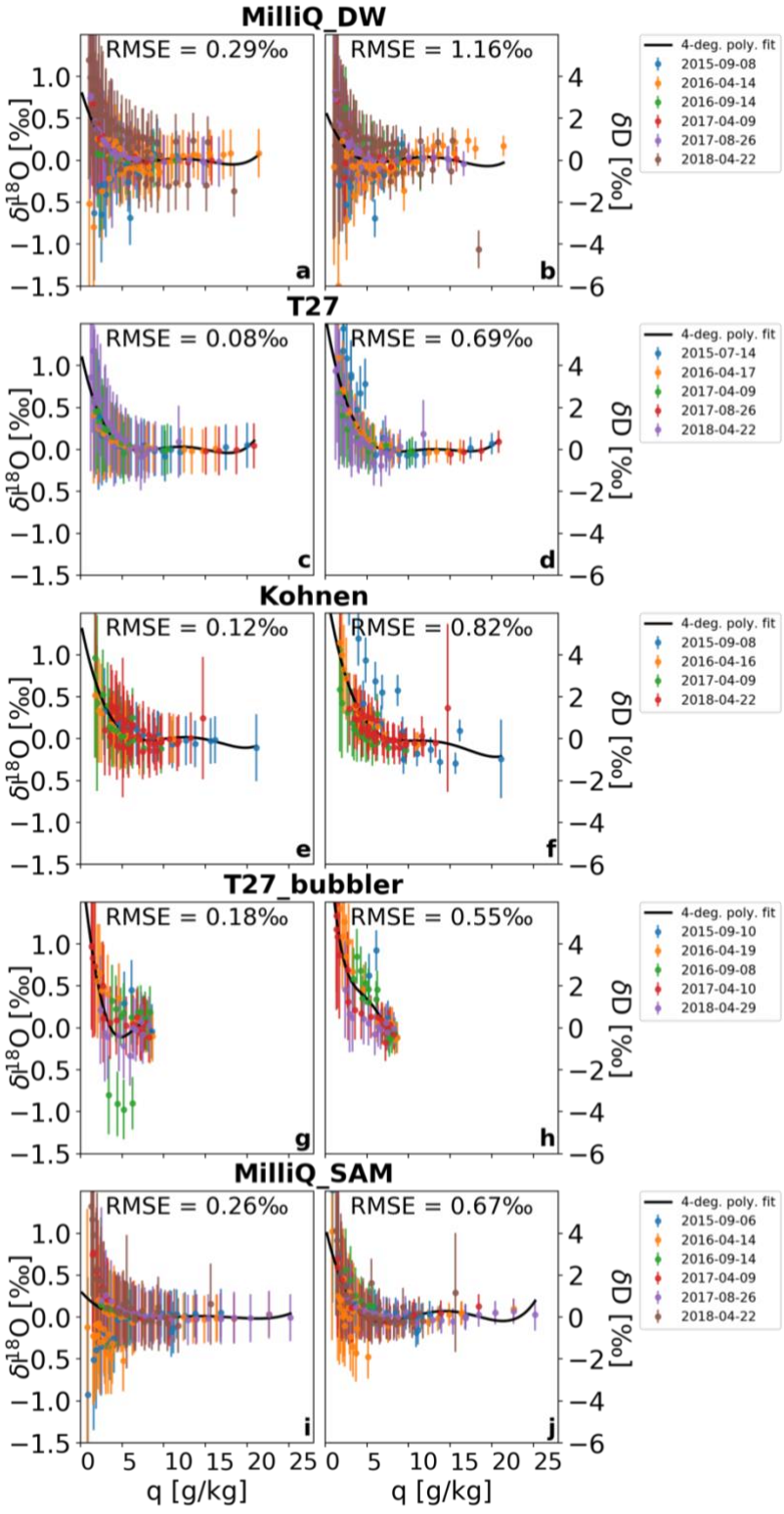

Supplementary Figure 1**: Humidity response functions experiments for the water vapour isotopic analyser.** Humidity response functions experiments are presented as a deviation from the mean isotopic value between 10 000 and 25 000 ppm (6.2 to 15.5 g/kg). Each row corresponds to one individual standard: (a,b) MilliQ_DW, (c,d) T27, (e, f) Kohnen, (g,h) T27 measured with the bubbler system, (i,j) MilliQ_SAM. The functions are displayed for (a,c,e,g,i) $\delta^{18}O$ and (b,d,f,h,j) $\delta^{2}H$.

Measured values are displayed with dots as the mean value and vertical error bars representing the standard deviation of the isotopic value during the time of the injection. Successive experiments conducted at different periods are respectively presented in blue, orange, green, red and purple and brown. The calculated response functions are displayed for the range of encountered ambient air humidity values as plain black lines.

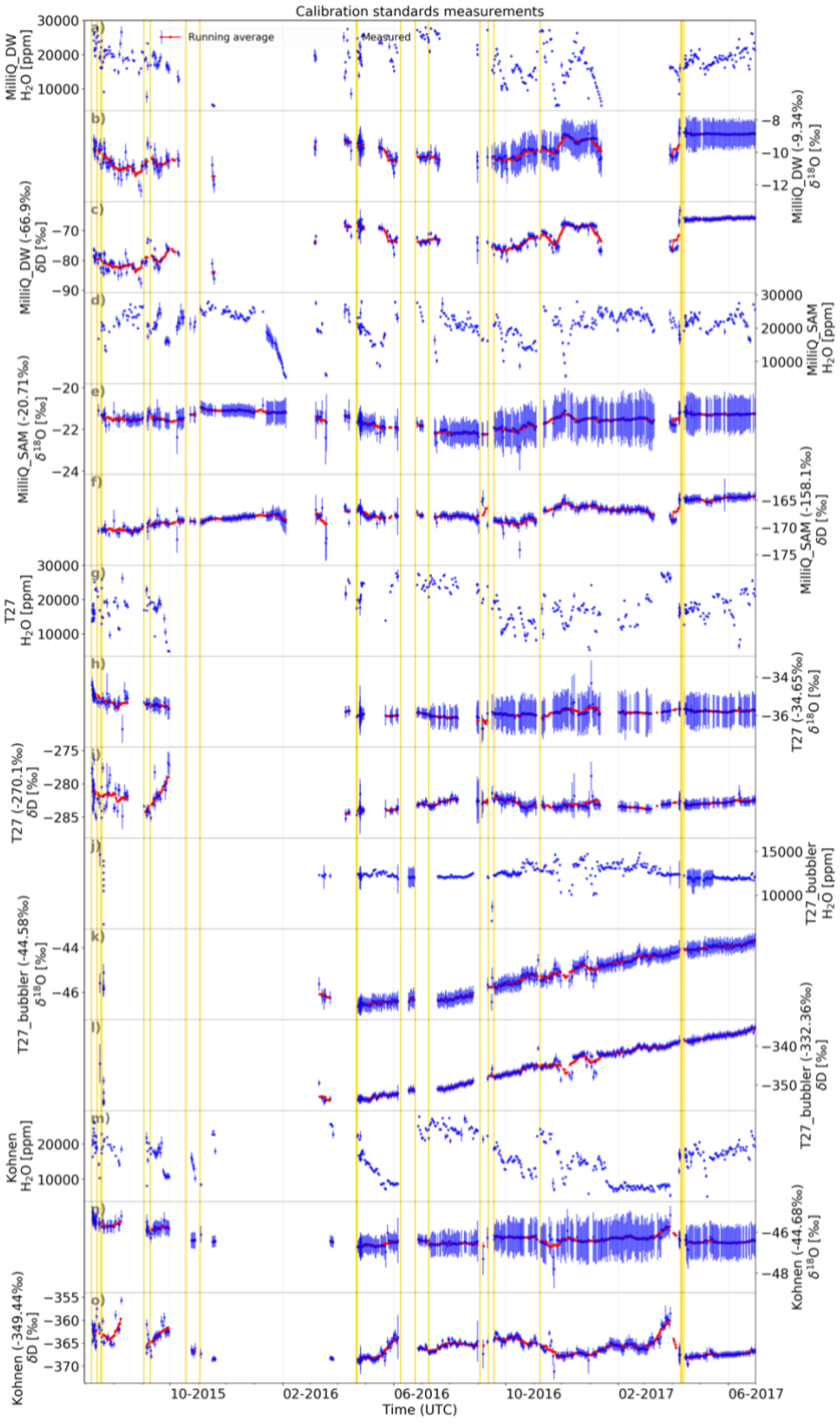

Supplementary Figure 2**: Measured isotopic values of the different calibration standards during the period 2015-06-29 to 2017-06-30.** The measurements of all different standards are successively displayed for the humidity level (in ppm), the $\delta^{18}O$ and the $\delta^{2}H$ corrected from humidity (in ‰): (a,b,c) MilliQ_DW, (d,e,f) MilliQ_SAM, (g,h,i) T27, (j,k,l) T27 measured with the bubbler system

and (m,n,o) Kohnen. Blue dots represent the mean and blue error bars represent standard deviation of the last 15 minutes of each 30-minute standard measurement. Outliers, which can be caused by instabilities of injections by the calibration system, have been removed from these data series. The red curves represent the 14-days running averages of these measurements, used for the computation of the calibration curves. The expected isotopic composition of each standard, as determined by independent laboratory measurements are given for each standard in the y-labels for $\delta^{18}O$ and the $\delta^{2}H$. Yellow vertical bars indicate the restarts of the Cavity Ringdown Spectrometer.

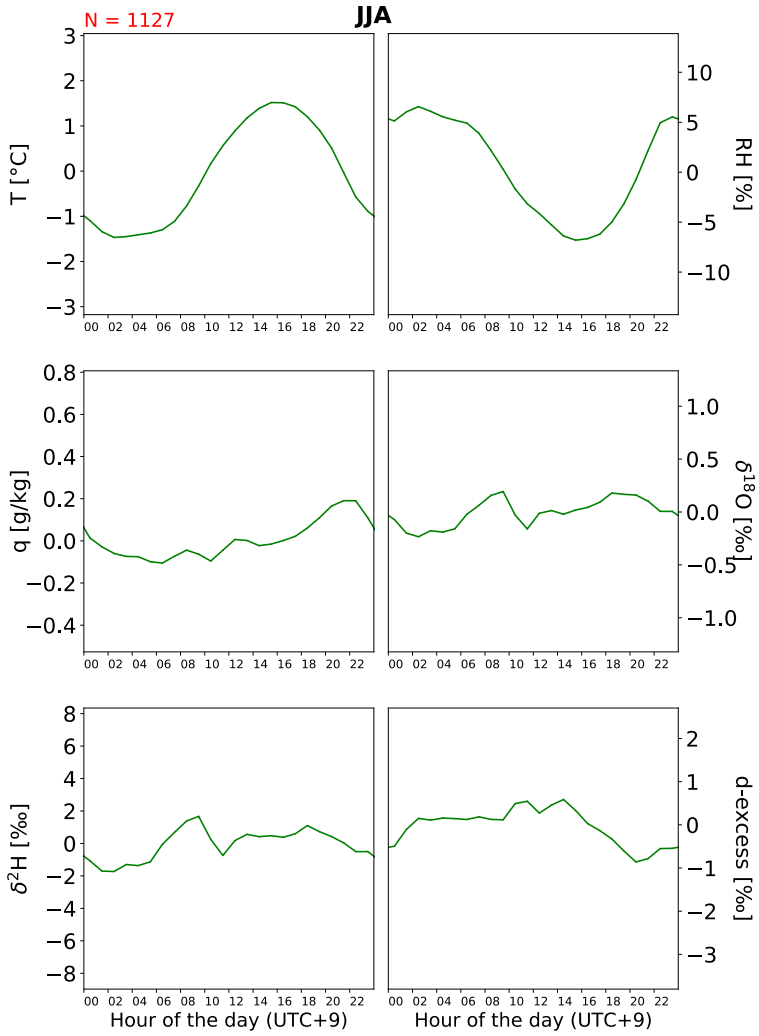

Supplementary Figure 3: Average daily cycle for summer season (June, July, August) for selected days of stable synoptic conditions (wind speed below 5 m.s-1 over 24 hours), for T (°C), RH (%), q (g/kg), $\delta^{18}O$ (‰), $\delta^{2}H$ (‰) and d-excess (‰). The daily cycles are calculated with the stacked anomalies compared to the daily average. The local time (UTC+9) is used to present to the results.

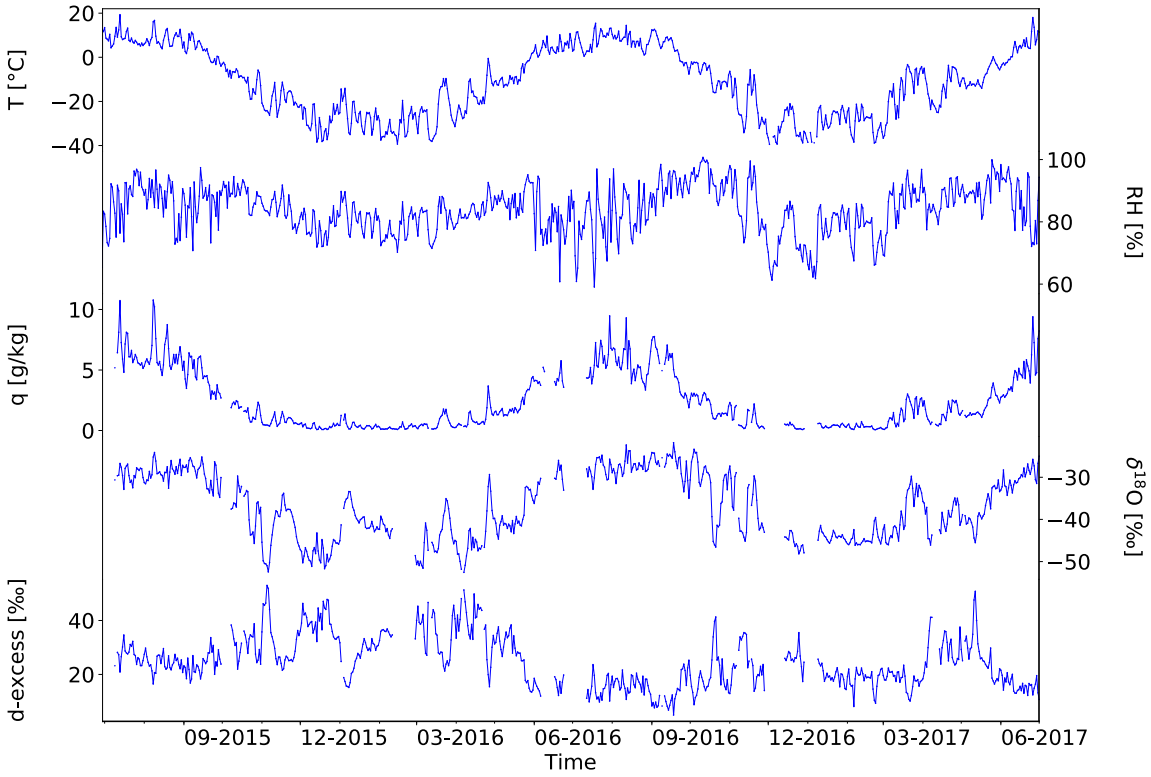

Supplementary Figure 4: Time series of ambient air observations at Samoylov for the period 2015-07-1 to 2017-07-01 at daily temporal resolution for air temperature (°C), relative humidity (%), specific humidity q (g kg-1), $\delta^{18}O$ *(‰) and d-excess (‰).*

Low temperatures	Low specific humidity	Low $\delta^{18}O$	High d-excess
2015-12-09	2015-12-09	2015-12-03	2015-12-03
2015-12-14	2015-12-14	2015-12-08	2015-12-15
2015-12-15	2015-12-15	2015-12-09	2015-12-17
2015-12-18	2015-12-18	2015-12-10	2015-12-19
2015-12-19	2015-12-19	2015-12-16	2015-12-20
2015-12-22	2015-12-22	2015-12-17	2015-12-21
2016-03-13	2016-03-13	2015-12-20	2015-12-22
2016-03-14	2016-03-14	2015-12-21	2015-12-23
2016-03-15	2016-03-15	2015-12-23	2016-03-02
2016-03-16	2016-03-16	2015-12-24	2016-03-10
2016-03-31	2016-03-31	2016-03-01	2016-03-30
2016-12-27	2016-12-27	2016-03-02	2016-04-05
2016-12-28	2016-12-28	2016-03-03	2016-04-07
2017-02-06	2017-02-06	2016-03-04	2016-04-08
2017-02-21	2017-02-21	2016-03-05	2016-04-15
2017-02-22	2017-02-22	2016-03-06	2016-04-18
2017-02-23	2017-02-23	2016-04-04	2016-04-19
2017-02-24	2017-02-24	2016-04-05	2016-04-20
2017-02-25	2017-02-25	2016-04-07	2016-04-21
2017-02-28	2017-02-26	2016-04-08	2016-12-25
2017-03-01	2017-02-28	2016-04-09	2017-04-06
2017-03-02	2017-03-01	2017-03-05	2017-04-07
2017-03-03	2017-03-02	2017-04-05	2017-04-08
2017-04-07	2017-03-03	2017-04-06	2017-04-18
2017-04-14	2017-03-04	2017-04-07	2017-04-19
2017-04-15	2017-03-11	2017-04-08	2017-04-30

Supplementary Table 1: Dates of the selected synoptic events of low temperature, low specific humidity, low $\delta^{18}O$ and high d-excess

High Temperature	High specific humidity	High $\delta^{18}O$	Low d-excess
2016-01-02	2016-01-02	2016-01-04	2016-01-04
2016-01-04	2016-01-04	2016-01-05	2016-01-05
2016-01-05	2016-01-05	2016-01-06	2016-01-06
2016-01-11	2016-01-06	2016-01-07	2016-01-07
2016-01-12	2016-01-11	2016-01-08	2016-01-08
2016-03-19	2016-01-12	2016-01-09	2016-01-09
2016-03-20	2016-03-20	2016-01-10	2016-01-10
2016-03-21	2016-03-21	2016-01-11	2016-01-11
2016-03-22	2016-03-22	2016-03-22	2016-01-12
2016-03-23	2016-03-23	2016-03-23	2016-03-19
2016-03-24	2016-03-24	2016-03-24	2016-03-21
2016-03-25	2016-03-25	2016-03-25	2016-03-22
2016-04-12	2016-04-26	2016-03-26	2016-03-23
2016-04-26	2016-04-27	2016-03-27	2016-03-24
2016-04-27	2017-01-28	2016-04-26	2016-03-25
2017-03-15	2017-02-12	2016-04-27	2016-03-26
2017-03-16	2017-03-15	2016-04-28	2016-03-27
2017-03-19	2017-03-19	2017-03-20	2016-04-25
2017-03-20	2017-03-20	2017-03-21	2016-04-26
2017-03-21	2017-03-21	2017-03-22	2016-04-27
2017-03-22	2017-03-22	2017-03-23	2016-04-28
2017-03-23	2017-03-23	2017-03-24	2017-02-06
2017-03-26	2017-03-26	2017-03-26	2017-02-23
2017-03-27	2017-03-27	2017-03-27	2017-03-21
2017-03-30	2017-03-30	2017-03-29	2017-03-22
2017-03-31	2017-03-31	2017-03-30	2017-03-23

Supplementary Table 2: Dates of the selected synoptic events of high temperature, high specific humidity, high $\delta^{18}O$ and low d-excess